Available online at www.sciencedirect.com
ScienceDirect
Journal of Fluorine Chemistry 128 (2007) 263–268
JOURNAL OF FLUORINE CHEMISTRY
www.elsevier.com/locate/fluor

Review

Impacts of fluorine on the electrochemical properties of $Li[Ni_{0.5}Mn_{0.5}]O_2$ and $Li[Li_{0.2}Ni_{0.15}Co_{0.1}Mn_{0.55}]O_2$ ☆

K. Amine *, Zonghai Chen, S.-H. Kang

Electrochemical Technology Program, Chemical Engineering Division, Argonne National Laboratory, Argonne, IL 60439, USA

Received 1 September 2006; received in revised form 26 October 2006; accepted 30 October 2006
Available online 6 November 2006

Abstract

The impact of the fluorine substitution on the electrochemical properties of layered lithium nickel manganese positive electrode materials for lithium ion batteries is summarized. The addition of a controlled amount of fluorine to the oxygen lattice can effectively improve the capacity retention as well as reduce the impedance of the positive electrode materials. The fluorination of the nickel and manganese based layered oxide cathode material has also led to significant improvement in cycle life and power capability of the battery.

Keywords: Lithium-ion battery; Positive electrode materials; Fluorination

Contents

1. Introduction

Currently, $LiCoO_2$ is the predominant cathode material for lithium-ion batteries because of its ease of preparation and stable electrochemical cycling performance. Concerns about the high cost of cobalt and the safety characteristics of the batteries have led to the development of alternative cathode materials that offer low cost, high energy density, longer life, and improved abuse tolerance. A major development effort has been focused on optimizing the $Li[Mn_{1-x-y}Ni_xCo_y]O_2$ system to improve the battery performance [1–4]. For instance, Dahn et al. have devoted considerable effort to understanding the structure, electrochemical properties, and safety issues of a series of new materials, $Li[Ni_xCo_{1-2x}Mn_x]O_2$ ($0 \leq x \leq 1/2$) [5–10]. In this case, the electronic configuration of Mn^{4+}, Ni^{2+}, and Co^{3+} is energetically preferred compared to that of Mn^{3+}, Ni^{3+}, and Co^{3+}. Therefore, the manganese stays as Mn^{4+} during the charge/discharge cycling, and the detrimental impact of Jahn–Teller distortion associated with Mn^{3+} can be avoided. Moreover, it was also reported that $Li[Ni_xCo_{1-2x}Mn_x]O_2$ ($x > 0.2$) charged to 4.4 V showed better thermal stability in the

☆ The submitted manuscript has been created by UChicago Argonne, LLC, Operator of Argonne National Laboratory (“Argonne”). Argonne, a U.S. Department of Energy Office of Science Laboratory, is operated under Contract No. DE-AC02-06CH11357. The U.S. Government retains for itself, and others acting on its behalf, a paid-up nonexclusive, irrevocable worldwide license in said article to reproduce, prepare derivative works, distribute copies to the public, and perform publicly and display publicly, by or on behalf of the government.

* Corresponding author.
E-mail address: amine@cmt.anl.gov (K. Amine).

0022-1139/$ – see front matter © 2006 Elsevier B.V. All rights reserved.
doi:10.1016/j.jfluchem.2006.10.017

non-aqueous electrolyte than $Li_{0.5}CoO_2$ [6]. Meanwhile, the transition metals in the positive electrode materials can also be replaced with other metallic elements, which maintain only one valence state during the charge/discharge process. It has been widely reported that such fixed-valence-state elements, such as Al [11–13], Cr [14–16], Mn, greatly improved the electrochemical performances of the positive electrode materials. Special attention was also paid to the lithium-doped materials due to its several advantages [2,14,17–22]. Li^+ has the lowest valence state among the metallic elements and can effectively raise the valence state of the transition metals to stabilize the performance of the positive electrode materials. Furthermore, Li has the smallest atomic weight and such substitution results in limited decrease in the specific capacity. Finally, the extra capacity delivered at about 4.5 V versus Li^+/Li can be very attractive for high-energy lithium-ion batteries [17].

Besides the widely reported cation substitution mentioned above, there has been an active effort at Argonne National Laboratory to study the impact of the anion substitution, such as replacing part of the oxygen with fluorine. In this paper, we report that the fluorine substitution can effectively improve the electrochemical performances of the $Li(Ni_{0.5+0.5z}Mn_{0.5-0.5z})O_{2-z}F_z$ and $Li[Li_{0.2}Ni_{0.15+0.5z}Co_{0.10}Mn_{0.55-0.5z}]O_{2-z}F_z$ metal oxides that are very promising cathode materials for high energy, long cycle life and better abuse tolerance lithium ion batteries.

2. Impact of fluorination on crystal structures

Fig. 1 shows the XRD patterns of $Li(Ni_{0.5+0.5z}Mn_{0.5-0.5z})O_{2-z}F_z$ with different degrees of fluorination. The diffraction patterns of the synthesized samples can be indexed based on the α-$NaFeO_2$-type structure ($R\bar{3}mo$). Fig. 1 shows that the relative intensity of (0 0 3) to (1 0 4) peaks ($I_{(0\,0\,3)}/I_{(1\,0\,4)}$) decreased from 1.29 ($z = 0$) to 0.607 ($z = 0.2$) and the splitting of (0 0 6)/(1 0 2) and (0 1 8)/(1 1 0) peaks became less pronounced with the increase in the amount of fluorine. The changes on the XRD patterns indicate that the degree of cation disorder increases and the crystal structure becomes closer to cubic with increasing fluorine content. Fig. 2 shows an example of the Rietveld refinement for the composition of $Li(Ni_{0.51}Mn_{0.49})O_{1.8}F_{0.02}$. When the fluorine content increase, the lattice parameters increased from $a = 2.8862$ Å and $c = 14.292$ Å for $z = 0$ to $a = 2.9000$Å and $c = 14.314$Å for $z = 0.2$; at the same time Li occupancy in the transition metal layer (or Ni occupancy in the lithium layer) increased from 0.0585 for $z = 0$ to 0.1376 for $z = 0.2$, which explains the decrease of $I_{(0\,0\,3)}/I_{(1\,0\,4)}$ ratio with increasing z values. Fig. 3 shows the XRD

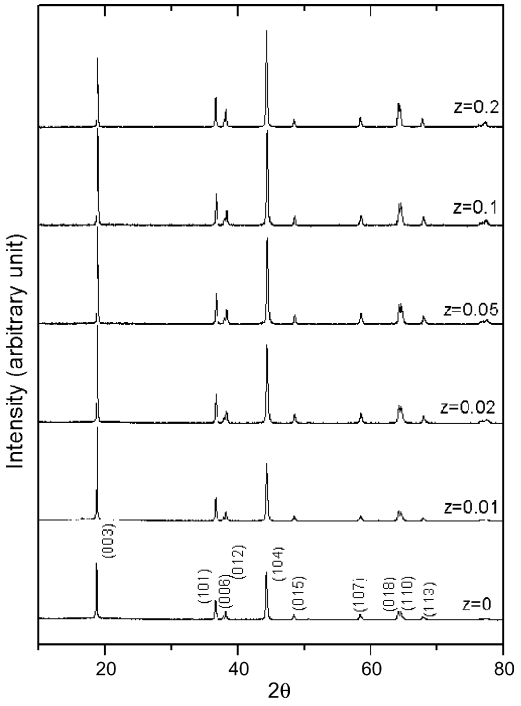

Fig. 1. XRD patterns of $Li(Ni_{0.5+0.5z}Mn_{0.5-0.5z})O_{2-z}F_z$ ($0 \le z \le 0.2$) calcined at 1000 °C for 15 h in air.

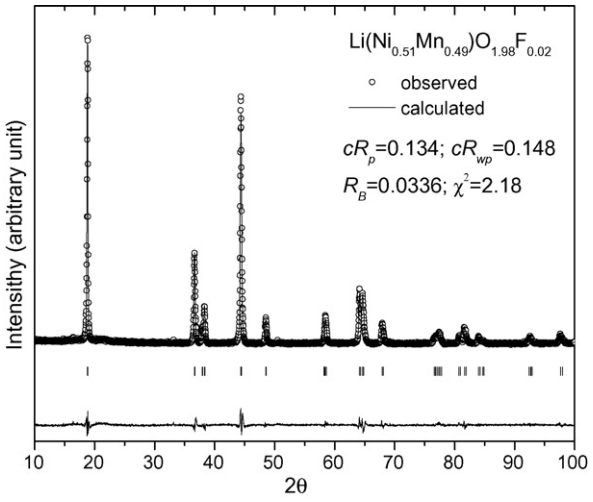

Fig. 2. The Rietveld refinement results for $Li(Ni_{0.51}Mn_{0.49})O_{1.98}F_{0.02}$.

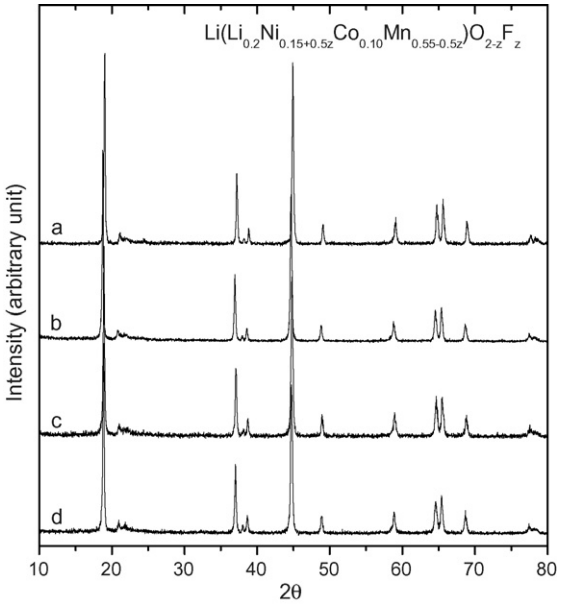

Fig. 3. XRD patterns of $Li[Li_{0.2}Ni_{0.15+0.5z}Co_{0.10}Mn_{0.55-0.5z}]O_{2-z}F_z$. (a) $z = 0$; (b) $z = 0.02$; (c) $z = 0.05$; (d) $z = 0.10$.

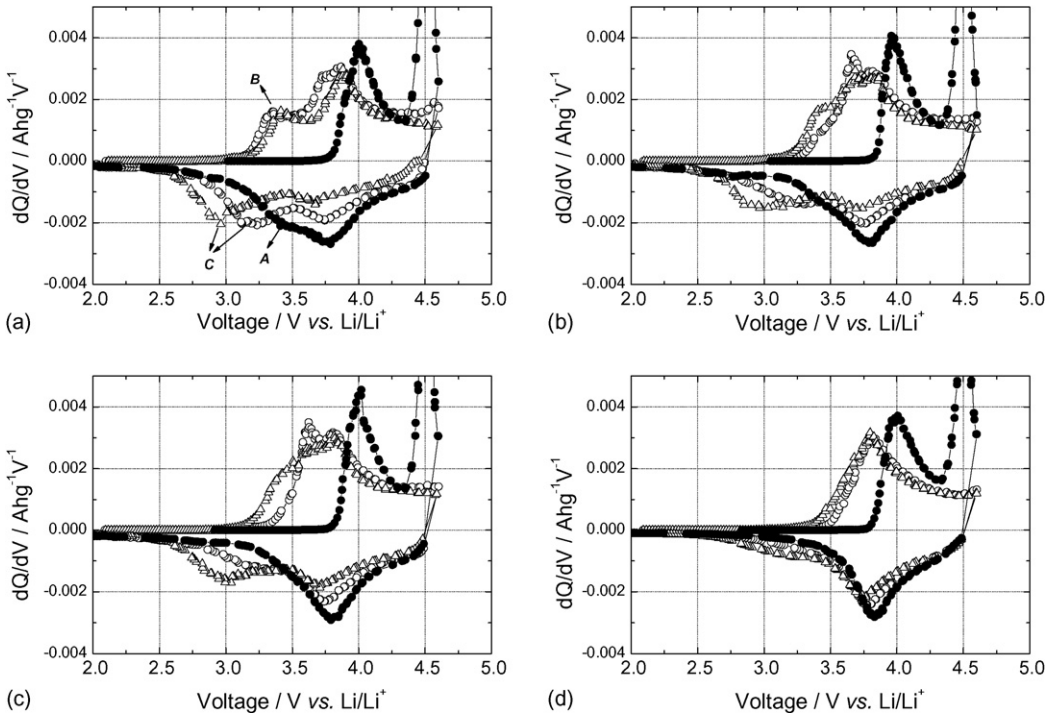

Fig. 4. Differential capacity *vs.* voltage of Li/Li[$Li_{0.2}Ni_{0.15+0.5z}Co_{0.10}Mn_{0.55-0.5z}$]$O_{2-z}F_z$ cells cycled at 2.0–4.6 V. (a) $z = 0$; (b) $z = 0.02$; (c) $z = 0.05$; (d) $z = 0.10$. Solid circles, open circles, and open triangles denote the 1st, 10th, 40th cycle, respectively.

patterns of Li[$Li_{0.2}Ni_{0.15+0.5z}Co_{0.10}Mn_{0.55-0.5z}$]$O_{2-z}F_z$. The diffraction patterns of the synthesized samples could be indexed based on the α-$NaFeO_2$–type structure ($R\bar{3}m$) with small extra peaks at 20–23°, which are generally attributed to ordering of Li and Mn in the transition-metal layers. Generally, the structure of the fluorinated materials remained on the α-$NaFeO_2$-type structure ($R\bar{3}m$) with slight increases on the lattice parameters, and the cation mixing between Li and Ni increases with the content of fluorine.

3. Impact of fluorination on electrochemical reactions

Fig. 4 shows the differential capacity profiles of Li/Li[$Li_{0.2}Ni_{0.15+0.5z}Co_{0.10}Mn_{0.55-0.5z}$]$O_{2-z}F_z$ half cells. The solid circles represent the data for the first cycle, open circles represent the 10th cycle, and the open triangles represent the 40th cycle. The extra peak at about 4.4 V versus Li^+/Li was observed for all the samples regardless of the content of fluorine. This peak is attributed to the removal of the excess lithium in the metal site of the positive electrode materials. Fig. 4a shows several features that are related to the lithium-excess materials; (1) a shoulder was observed at about 3.4 V (marked as A) during the first discharge; (2) an extra pair of reversible peaks was observed between 3.0 V (marked as C) and 3.4 V (marked as B), and this pair of peaks were absent from the initial charge/discharge cycle. With the introducing of fluorine in the material lattice, the extra peaks were greatly suppressed. As the fluorine content increased, the additional differential capacity peaks marked as A, B, and C became less clear. We believe that the doped fluorine atoms prefer to occupy those oxygen sites that are neighboring the lithium atoms in the transition metal sites. In a lithium-doped materials, the average valence state of the transition metal at the charged state is +4 while the doped lithium in the transition metal layer remains at +1. Therefore, there will be local charge unbalance around the doped lithium atom, and the charge balance in a bigger area can be achieved by pinning down 3 more lithium ions in the lithium layer to compensate for the charge difference between Li^+ and tetravalent metal. These pinned lithium clusters can be accessed at a high potential, i.e. 4.4 V versus Li^+/Li or higher, while generating defects on the oxygen lattice. This hypothesis could explain the electrochemical behavior described in Fig. 4a. If the doped fluorine first occupies the oxygen lattice next to the doped lithium, the local pairing of Li^+–F^- can greatly alleviated the local charge unbalance, and the unusual behavior of lithium-doped materials as shown in Fig. 4a can be suppressed. To further corroborate this hypothesis, experiment using solid-state nuclear magnetic resonance (NMR) is under way and the result will be published in the future.

4. Impact of fluorination on capacity retention

Fig. 5 shows the variation of discharge capacity of the Li/Li($Ni_{0.5+0.5z}Mn_{0.5-0.5z}$)$O_{2-z}F_z$ cells cycled between 2.8 and 4.3 V. The initial capacity slightly increased with fluorine substitution up to $z = 0.02$ and then decreased afterwards, as is shown in the inset of Fig. 5. The capacity retention was also improved slightly by the small amount of fluorine substitution. However, both the initial capacity and the capacity retention suffered when the material was heavily doped with 20% fluorine. The materials described in Fig. 5 were specially formulated to maintain the valence state of Mn at tetravalent

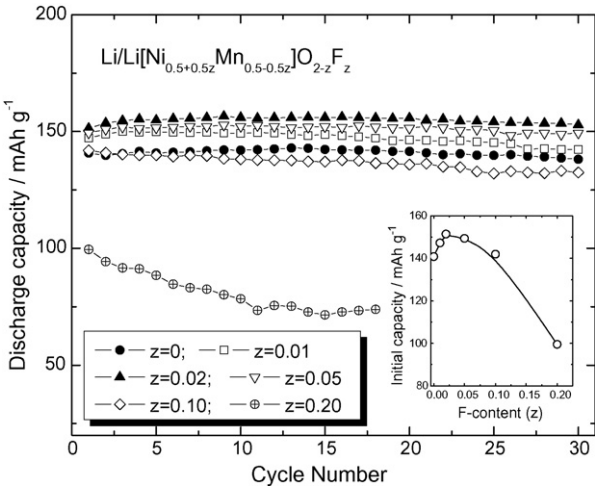

Fig. 5. Discharge capacity of $Li/Li(Ni_{0.5+0.5z}Mn_{0.5-0.5z})O_{2-z}F_z$ ($0 \le z \le 0.2$) cells with cycling in the voltage range of 2.8–4.3 V at a current density of 0.1 mA/cm^2 (~10 mA/g). In the inset is shown the initial discharge capacity as a function of fluorine content.

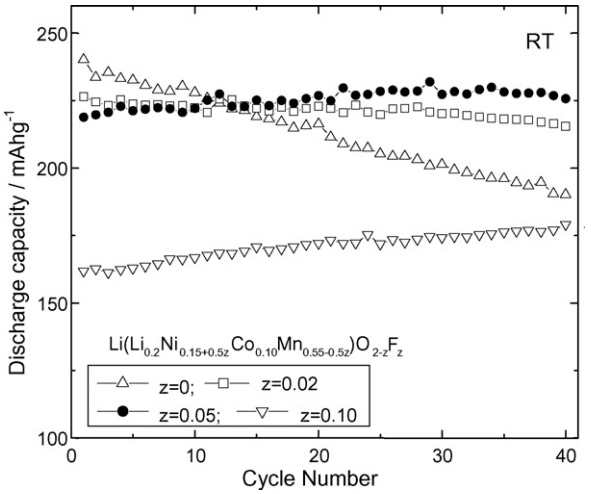

Fig. 7. Discharge capacity of $Li/Li[Li_{0.2}Ni_{0.15+0.5z}Co_{0.10}Mn_{0.55-0.5z}]O_{2-z}F_z$ cells cycled in the voltage range of 2.0–4.6 V at room temperature.

state. However, one might raise a question whether the improvement was caused solely by the fluorine doping or by the change of the ratio of Ni to Mn ratio in the transition metal layer. Fig. 6 shows the discharge capacity of the three electrode materials as a function of cycle number. The cell based on $Li(Ni_{0.51}Mn_{0.49})O_2$ delivered almost the same initial capacity as $Li(Ni_{0.51}Mn_{0.49})O_{1.98}F_{0.02}$ based cell, possibly due to the increase in the electrochemically active nickel content. However, $Li(Ni_{0.51}Mn_{0.49})O_2$ exhibited poor capacity retention than $Li(Ni_{0.51}Mn_{0.49})O_{1.98}F_{0.02}$ Therefore, we concluded that the improvement on the capacity retention is due to the fluorine substitution.

Fig. 7 shows the capacity retention of another series of materials $Li(Li_{0.2}Ni_{0.15+0.5z}Co_{0.10}Mn_{0.55-0.5z})O_{2-z}F_z$, which have 20% excess lithium in the transition metal layer. These cells were cycled between 2.8 and 4.6 V at room temperature. The material without doped fluorine had the highest initial discharge capacity, but the capacity retention for this material was very poor (losing about 25% initial capacity after 40 cycles at room temperature). When 2% fluorine was added to the oxygen sites, the material had a slightly lower initial discharge capacity (about 225 mAh/g), and no capacity fade was observed up to 40 cycles. It is also clear that the initial discharge capacity of the materials greatly suffered when more than 5% fluorine was doped. An activation process was also observed for the materials with high fluorine content, i.e. $z = 0.10$. It is possible that the full discharge capacity of $Li(Li_{0.20}Ni_{0.20}Co_{0.10}Mn_{0.5})O_{1.9}F_{0.1}$ ($z = 0.10$) was not reached after only 40 cycles, and the actual capacity retention of this material can only be accessed for longer test period. Alternatively, the evaluation can be carried out at a higher temperature to accelerate the activation process. Fig. 8 shows the capacity retention of $Li/Li(Li_{0.20}Ni_{0.15+0.5z}Co_{0.10}Mn_{0.55-0.5z})O_{2-z}F_z$ ($z = 0$, 0.02, 0.05, and 0.10, respectively) at 55 °C. Clearly, the activation process for the high-fluorine-content materials was completed in less than five cycles. The material with high fluorine content ($z = 0.10$) has a lower initial discharge capacity. Fig. 8 clearly shows that the capacity retention of this series of materials increase with the content of fluorine. When 10% fluorine was added, the material

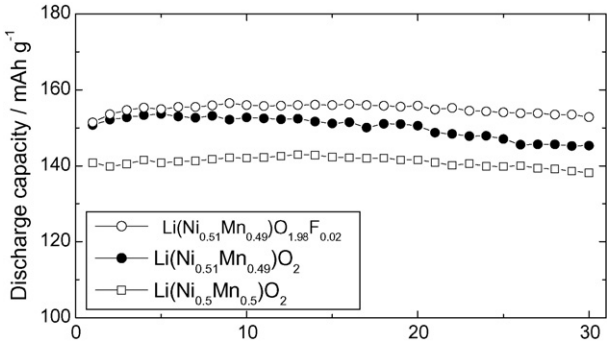

Fig. 6. Discharge capacity of $Li(Ni_{0.5}Mn_{0.5})O_2$ and $Li(Ni_{0.51}Mn_{0.49})O_{2-z}F_z$ ($z = 0$, 0.02) measured against Li metal and graphite, respectively, as a function of cycle number.

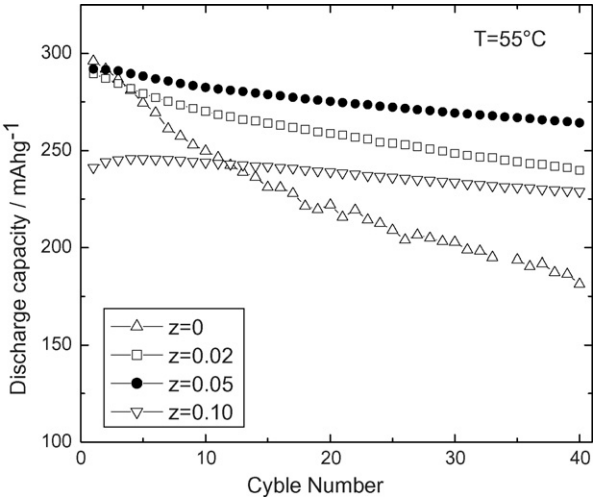

Fig. 8. Discharge capacity of $Li/Li[Li_{0.2}Ni_{0.15+0.5z}Co_{0.10}Mn_{0.55-0.5z}]O_{2-z}F_z$ cells in the voltage range of 2.0–4.6 V as a function of cycle number at 55 °C.

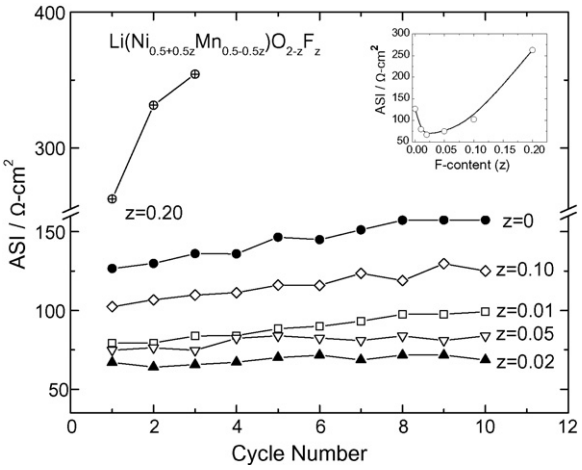

Fig. 9. ASI at 50% SOC of C/Li($Ni_{0.5+0.5z}Mn_{0.5-0.5z}$)$O_{2-z}F_z$ cells as a function of the cycle number. Change of the initial ASI values at 50% SOC with fluorine content is given in the inset.

delivered a reversible capacity of about 250 mAh/g, and no capacity fade was observed after 40 cycles at 55 °C.

5. Impact of fluorination on area specific impedance

Fig. 9 shows the area specific impedance (ASI) at 50% state-of-charge (SOC) as a function of the cycle number of for graphite/Li($Ni_{0.5+0.5z}Mn_{0.5-0.5z}$)$O_{2-z}F_z$ cells. The ASI, characterizing the power performance of the Li-ion cells, was determined by $A\,\Delta V/I$, where A is the cross sectional area of the electrodes, ΔV the voltage change during current interruption for 30 s, and I is the current applied during the galvanostatic cycling. Fig. 9 shows that the initial ASI decreased significantly up to $z = 0.02$ (127 Ω cm^2 for $z = 0$ and 67 Ω cm^2 for $z = 0.02$), and then increased rapidly afterwards. As can be seen in Fig. 9, the fluorine content also affected the ASI growth during cycling; with $Li(Ni_{0.51}Mn_{0.49})O_{1.98}F_{0.02}$ showed lower ASI than other materials.

Fig. 10 shows the average ASI at 60–80% state of charge (SOC) of graphite/Li[$Li_{0.2}Ni_{0.15+0.5z}Co_{0.10}Mn_{0.55-0.5z}$]$O_{2-z}F_z$

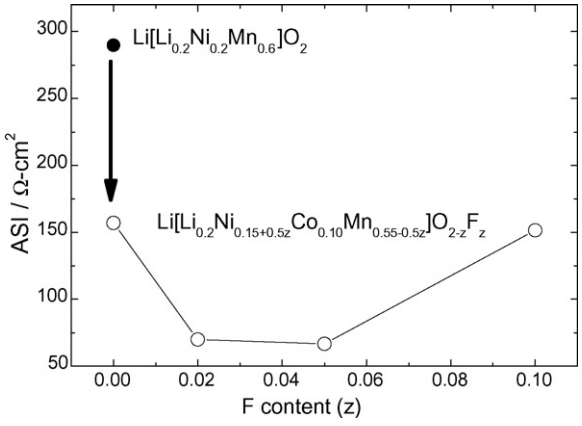

Fig. 10. Average area specific impedance (ASI) at 60–80% state of charge (SOC) measured with graphite/Li[$Li_{0.2}Ni_{0.15+0.5z}Co_{0.10}Mn_{0.55-0.5z}$]$O_{2-z}F_z$ cells as a function of fluorine content. The solid circle is the ASI measured with graphite/Li[$Li_{0.2}Ni_{0.2}Mn_{0.6}$]O_2 cell.

cells. The ASI for the graphite/Li[$Li_{0.2}Ni_{0.2}Mn_{0.6}$]O_2 cell is also shown in Fig. 10. When adding 10% Co to Li[$Li_{0.2}Ni_{0.2}Mn_{0.6}$]O_2, the ASI drops significantly from 290 to 150 Ω cm^2. This is because cobalt trivalent induce a mix valence in the system resulting in the increase in the electrical conductivity of the material [23]. However, when adding less than 5% fluorine to the material, the impedance of the material was further lowered to as low as 65 Ω cm^2 for $Li(Li_{0.2}Ni_{0.175}Co_{0.1}Mn_{0.525})O_{1.95}F_{0.05}$.

6. Conclusions

The impact of fluorine doping on the electrochemical properties of layered positive electrode materials was summarized using $Li(Ni_{0.5+0.5z}Mn_{0.5-0.5z})O_{2-z}F_z$ $(0 \le z \le 0.1)$ and $Li[Li_{0.2}Ni_{0.15+0.5z}Co_{0.10}Mn_{0.55-0.5z}]O_{2-z}F_z$ $(0 \le z \le 0.10)$ as examples. The initial capacity of the doped materials can be slightly improved with a small amount of doped fluorine. In addition, a controlled amount of doped fluorine can also improve the capacity retention, initial power capability and the power retention of the layered lithium nickel manganese positive electrode materials. Generally, 2–5% fluorine is recommended for better performance. The combination of cation substitution and anion substitution can be the effective way to stabilize the positive electrode materials and improve it cycling and safety performance. The local pairing of Li^+–F^- cluster was proposed to explain the behavior changes observed in the dQ/dV plots in the materials with both lithium and fluorine-doping.

Acknowledgements

The authors acknowledge the financial support of the U.S. Department of Energy, FreedomCAR & Vehicle Technologies Program, under contract No. DE-AC02-06CH11357.

References

[1] A.N. Mansour, L. Croguennec, C. Delmas, Electrochem. Solid-State Lett. 8 (2005) A544–A548.
[2] N. Tran, L. Croguennec, C. Labrugere, C. Jordy, P. Biensan, C. Delmas, J. Electrochem. Soc. 153 (2006) A261–A269.
[3] I. Saadoune, C. Delmas, J. Solid State Chem. 136 (1998) 8–15.
[4] D. Carlier, M. Menetrier, C. Delmas, J. Mater. Chem. 11 (2001) 594–603.
[5] D.D. Macneil, Z. Lu, J.R. Dahn, J. Electrochem. Soc. 149 (2002) A1332–A1336.
[6] J. Jiang, K.W. Eberman, L.J. Krause, J.R. Dahn, J. Electrochem. Soc. 152 (2005) A566–A569.
[7] S. Jouanneau, K.W. Eberman, L.J. Krause, J.R. Dahn, J. Electrochem. Soc. 150 (2003) A1637–A1642.
[8] S. Jouanneau, D.D. Macneil, Z. Lu, S.D. Beattie, G. Murphy, J.R. Dahn, J. Electrochem. Soc. 150 (2003) A1299–A1304.
[9] S. Jouanneau, W. Bahmet, K.W. Eberman, L.J. Krause, J.R. Dahn, J. Electrochem. Soc. 151 (2004) A1789–A1796.
[10] S. Jouanneau, J.R. Dahn, J. Electrochem. Soc. 151 (2004) A1749–A1754.
[11] J. Kim, B.H. Kim, Y.H. Baik, P.K. Chang, H.S. Park, K. Amine, J. Power Sources 158 (2006) 641–645.
[12] H.J. Bang, H. Joachin, H. Yang, K. Amine, J. Prakash, J. Electrochem. Soc. 153 (2006) A731–A737.
[13] C.H. Chen, J. Liu, M.E. Stoll, G. Henriksen, D.R. Vissers, K. Amine, J. Power Sources 128 (2004) 278–285.
[14] Z.H. Lu, Z.H. Chen, J.R. Dahn, Chem. Mater. 15 (2003) 3214–3220.

[15] Z.H. Lu, J.R. Dahn, J. Electrochem. Soc. 149 (2002) A1454–A1459.
[16] Z.H. Lu, J.R. Dahn, J. Electrochem. Soc. 150 (2003) A1044–A1051.
[17] Z.H. Lu, J.R. Dahn, J. Electrochem. Soc. 149 (2002) A815–A822.
[18] Z.H. Lu, L.Y. Beaulieu, R.A. Donaberger, C.L. Thomas, J.R. Dahn, J. Electrochem. Soc. 149 (2002) A778–A791.
[19] Z.H. Chen, K. Amine, J. Electrochem. Soc. 153 (2006) A1279–A1283.
[20] Z. Chen, Y.-K. Sun, K. Amine, J. Electrochem. Soc. 153 (2006) A1818–A1822.
[21] F. Tournadre, L. Croguennec, I. Saadoune, F. Weill, Y. Shao-Horn, P. Willmann, C. Delmas, Chem. Mater. 16 (2004) 1411–1417.
[22] F. Tournadre, L. Croguennec, I. Saadoune, M. Morcrette, P. Willmann, C. Delmas, Chem. Mater. 16 (2004) 1418–1426.
[23] S.H. Kang, J. Kim, M.E. Stoll, D. Abraham, Y.K. Sun, K. Amine, J. Power Sources 112 (2002) 41–48.